Experimental and Modeling Study on Tubular Dense Membranes for Oxygen Permeation

Nanping Xu, Shiguang Li, Wanqin Jin, and Jun Shi
Membrane Science & Technology Research Center, Nanjing University of Chemical Technology, Nanjing 210009, P.R. China

Y. S. Lin
Dept. of Chemical Engineering, University of Cincinnati, Cincinnati, OH 45221

Tubular $La_{0.6}Sr_{0.4}Co_{0.2}Fe_{0.8}O_{3-\delta}$ perovskite-type membranes were prepared by isostatic pressing. A mathematical model was developed to simulate the performance of the tubular perovskite-type dense membranes for oxygen permeation. The experimental oxygen permeation fluxes of tubular $La_{0.6}Sr_{0.4}Co_{0.2}Fe_{0.8}O_{3-\delta}$ perovskite-type membrane increased with decreasing downstream oxygen partial pressure and increasing helium flow rate, which coincided with the results of the oxygen permeation modeling study. Parametric study indicated that air should be supplied sufficiently during the oxygen permeation operation. Modeling oxygen permeation fluxes as a function of the tubular membrane length and tubular membrane thickness are discussed in detail. The oxygen flux slightly decreased after long-term operation over 110 h. EDS and XRD analysis indicated that $SrSO_4$, $CoSO_4$, SrO, Co_2O_3, and La_2O_3 were formed on the surfaces of the tubular membrane due to the interaction with trace SO_2 in the air and the helium, and segregation of surface elements. The oxygen permeation of tubular $La_{0.6}Sr_{0.4}Co_{0.2}Fe_{0.8}O_{3-\delta}$ membrane was stable after SO_2 in the air and the helium has been removed.

Introduction

Dense mixed-conducting ceramic membranes hold great promises for applications in separating oxygen from air and improving the performance of catalytic partial oxidation of hydrocarbons (Hsieh, 1996). Among them, perovskite-type oxide (ABO_3) containing a transition metal at B sites are found to be good materials that can be used as oxygen-semipermeable membranes without electrodes and external electrical circuits due to their high electronic and ionic conductivity (Lin et al., 1994). Teraoka et al. (1985) were the first to report very high oxygen fluxes through the cobalt-rich compositions, which are known to become highly oxygen defective because of the vacancy of the oxygen anions at elevated temperatures and a reduced oxygen partial pressure. Since then, increasing studies have been reported on the synthesis and properties of the $LaCoO_3$-based perovskite-type ceramics because of their potential applications as membranes in gas separation and membrane reactors (Gur et al., 1992; Itoh et al., 1994; van Hassel et al., 1993a,b, 1994; Kawada et al., 1995; Chen et al., 1997; ten Elshof et al., 1995a,b,c; Qiu et al., 1995; Kharton et al., 1996; Stevenson et al., 1996; Tsai et al., 1997; Lin and Zeng, 1996; Zeng et al., 1998; Li et al., 1998, 1999a,b). More details on recent developments in this area have been critically reviewed in two recent book chapters (Boumeester and Burggraaf, 1996, 1997).

For the dense perovskite-type membrane, the oxygen permeability is essentially controlled by two factors: the rate of bulk diffusion through the membrane and that of the surface reaction on either side of the membrane. Wagner's equation (Boumeester and Burggraaf, 1996) was used to describe the oxygen permeation flux through bulk diffusion as

$$J_{O_2} = \int_{P''_{O_2}}^{P'_{O_2}} \frac{1}{16F^2} \frac{RT\sigma_i\sigma_e}{(\sigma_i+\sigma_e)L} d\ln P_{O_2}, \qquad (1)$$

Correspondence concerning this article should be addressed to N. Xu.

where P'_{O_2}, P''_{O_2} (Pa) are the upstream and downstream oxygen partial pressures, respectively; σ_e and σ_i (S/cm) are the electronic conductivity and the ionic conductivity, respectively; R (J/mol·K) is the gas constant; F (C/mol) is the Faraday constant; T (K) is the temperature; L (cm) is the membrane thickness; and P_{O_2} (Pa) is the oxygen partial pressure. For perovskite-type membranes, the conductivity term can be simplified to be σ_i in the case of $\sigma_i \ll \sigma_e$. Many studies (Itoh et al., 1994; Stevenson et al., 1996; Tsai et al., 1997) further simplified Eq. 1 to be

$$J_{O_2} = \frac{RT\sigma_i}{16LF^2} \ln \frac{P'_{O_2}}{P''_{O_2}}, \tag{2}$$

assuming σ_i is independent of P_{O_2}. However, the oxygen ion or the oxygen vacancy concentration is dependent of P_{O_2} (Mizusaki et al., 1989; Boumeester and Burggraaf, 1996). The surface reaction of the perovskite-type membranes has also been studied by many researchers. Lee et al. (1997) proposed a model for the dependence of the surface exchange current on the chemical potential drop at the gas–solid interface, neglecting the dependence of the ion concentration in the solid on the gas pressure. Zeng and Lin (1998) demonstrated experimentally a simple and efficient TGA method to study the surface reaction rates for oxygen transport through thin mixed-conducting perovskite-type ceramic membranes.

Although many researchers have studied surface reaction and the bulk diffusion of the perovskite-type membranes, most work was focused on disk-shaped perovskite-type membranes and the effective area was very limited. Balachandran et al. (1995, 1997) appeared to be the only group that reported results on the tubular nonperovskite-type $SrFeCo_{0.5}O_{3-\delta}$ membrane by plastic extrusion. From the perspective of industrial applications, tubular membranes should be prepared. For the modeling study of the tubular dense membrane for oxygen permeation, in addition to coupling the surface reaction with the bulk diffusion, the solid–gas interface transfer resistance of oxygen transport should also be considered.

The purpose of this study was to investigate the oxygen permeability and long-term operation stability of tubular dense perovskite-type membranes. A mathematical model was developed to simulate the performance of the tubular perovskite-type dense membranes for oxygen permeation. The composition $La_{0.6}Sr_{0.4}Co_{0.2}Fe_{0.8}O_{3-\delta}$ was selected in this work because of its high oxygen permeability and good chemical stability among lanthanum cobaltite materials, as reported by Xu and Thomson (1998). The oxygen permeation experiments were conducted in a tubular membrane permeator. The element distribution and crystal structure of the tubular membrane after 110-h oxygen permeation were examined to study the membrane stability.

Experimental Studies

$La_{0.6}Sr_{0.4}Co_{0.2}Fe_{0.8}O_{3-\delta}$ powder was synthesized by a solid-state reaction of the constituent cationic salts (the Second Chemical Industry of Shanghai, purity of 99.9%). In the preparation of the oxide, appropriate amounts of La_2O_3, $Sr(CO_3)_2$, Co_2O_3, Fe_2O_3 were mixed with deionized water.

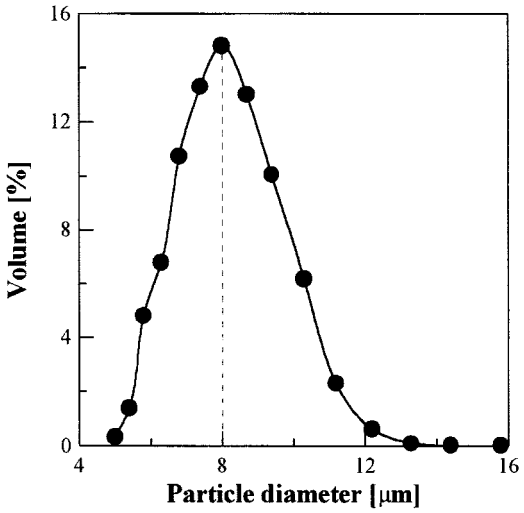

Figure 1. Particle-size distribution of the resulting $La_{0.6}Sr_{0.4}Co_{0.2}Fe_{0.8}O_{3-\delta}$ powders.

The mixture was ball-milled for 24 h by a ball grinder (Model QM-ISP, Nanjing University Experimental Industry, China) using two 250-mL stainless-steel tanks and stainless-steel balls with a rotation speed of 150 r/min. After being dried at 353 K for 24 h, the mixture was ground and sintered in air at 1,173 K for 5 h. The heating and cooling rates were controlled at 2 K/min. The process, including ball-milling, drying, and sintering, was repeated twice. The sintered powders were sifted and the particle sizes of the resulting powders were measured by a photo extinction sedimentation analyzer (Model NSKC-1A, Silicalite Engineering Research Center, Nanjing University of Chemical Technology, China). The particle-size distribution of the resulting powders is shown in Figure 1. As shown, the average particle size of the powders is about 8 μm.

In order to increase fluidity of the powder, PVA (10 wt. % in water) was added as an additive for the shaping process. After grinding, the powder was sifted to an average particle size between 40 and 60 mesh. Membrane tubes were prepared by isostatic pressing at the pressure of 25 MPa, which included loading, pressing, and ejecting. The green tubes were sintered in air at 1,523 K for 5 h in a $MoSi_2$ furnace at a heating and cooling rate of 3 K/min and 2 K/min, respectively. The final tubular membranes were 8 mm in outer diameter, 15 cm in length, and 1.5 mm in wall thickness.

Element analysis of the membranes was performed by energy-dispersive spectroscopy (EDS) (U.S. Kevex-Sigma). The densities of the sintered membranes were determined by the Archimedes method. All the membranes had densities at least 90% of the theoretical density.

Figure 2 shows the oxygen permeator used in this work for oxygen permeation measurement. The tubular membrane was mounted on an alumina tube surrounded by a quartz tube. The permeator was heated by a tubular furnace whose temperature could be controlled within ± 1°C by a microprocessor (Model 708PA, Xiamen Yuguang Electronics Technology Research Institute, China). A type K thermocouple encased in an alumina tube was used to measure the operation temperature. A ceramic binder developed in our laboratory was

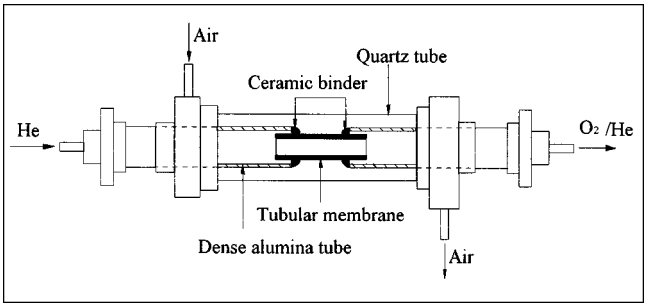

Figure 2. Oxygen permeator.

used to obtain an effective sealing between the wall of the tubular membrane and that of the alumina tube at high temperature. The ceramic binder contains alumina and some of the prepared perovskite-type oxide, so the coefficient of thermal expansion can be adjusted to meet the need of high-temperature sealing. The mounted membrane with the ceramic binder was first conditioned at 1,173 K for 30 min, then cooled to the desired temperature for oxygen permeation measurement at 2 K/min cooling rate. Experimental results (monitoring leakage of nitrogen) showed that the airtight sealing could be sustained at temperatures from 973 K to 1,173 K. A slight reaction between the membrane tube and the ceramic binder might be found at high temperatures, but it did not influence the operation of oxygen permeation.

The oxygen permeation rates through the tubular $La_{0.6}Sr_{0.4}Co_{0.2}Fe_{0.8}O_{3-\delta}$ membranes were measured on the permeation apparatus shown in Figure 3. The inlet gas flows were controlled by mass-flow controllers (Models D07-7A/ZM, Beijing Jianzhong Machine Factory, China). Air was introduced into the shell side of the permeator. Helium as the sweep gas for the permeating oxygen was fed to the tube side of the permeator. Both upstream and downstream gases were maintained at the atmospheric pressure. The effluent streams were analyzed by a gas chromatograph (Model Shimabzu GC-7A), which was equipped with a 2-m 5A molecular sieve operated at 40°C with H_2 as the carrier gas. The amount of oxygen passing through the membrane was calculated from

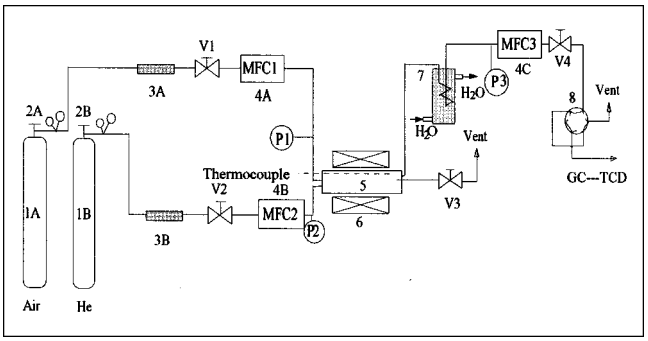

Figure 3. Apparatus used for the measurement of oxygen permeation rate.

(1A, 1B) gas cylinders; (2A, 2B) gas regulators; (3A, 3B) purifying traps; (4A, 4B, 4C) mass flow controller; (5) permeation reactor; (6) furnace; (7) cooler; (8) six-way valves; (V1–V4) flow control valves.

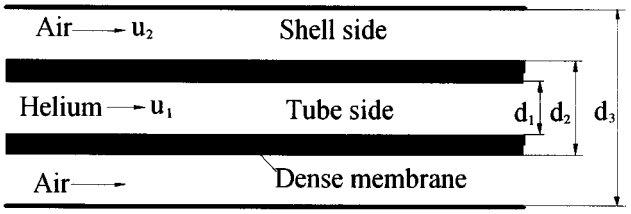

Figure 4. Cross section of the tubular membrane.

the helium flow rate, and the oxygen concentrations of the effluents.

Theoretical Model

In this section, a mathematical model in consideration of membrane bulk diffusion, membrane surface reaction, and solid–gas interface transfer resistance has been developed to simulate the performance of the tubular perovskite-type dense membranes for oxygen permeation. The cross section of the membrane is shown in Figure 4, where d_1, d_2, and d_3 are 0.5, 0.8, and 1.5 cm, respectively.

For membrane bulk diffusion, oxygen permeation through perovskite-type ceramic membranes can be given (Lin et al., 1994)

$$J_{O_2} = \frac{D_v}{2L}(C''_{v,b} - C'_{v,b}), \tag{3}$$

where D_v is the oxygen vacancy diffusivity of the membrane, and $C''_{v,b}$, $C'_{v,b}$ are the downstream and upstream oxygen vacancy concentration in membrane bulk at a given temperature, respectively.

For membrane surface reaction, the oxygen permeation flux can be described as

In tube side:

$$J_{O_2} = k_d(C''_{v,s} - C''_{v,b}) \tag{4}$$

In shell side:

$$J_{O_2} = k_a(C'_{v,b} - C'_{v,s}), \tag{5}$$

where k_d, k_a are, respectively, the desorption and absorption rate constants, and $C''_{v,s}$, $C'_{v,s}$ are the downstream and upstream oxygen vacancy concentration on membrane surfaces, respectively.

Combination of Eqs. 3, 4, and 5, and assuming that $C_v \propto P_{O_2}^{-m}$ (Zeng et al., 1998) gives

$$J_{O_2} = \frac{A\left(P''_{O_2 s}{}^{-m} - P'_{O_2 s}{}^{-m}\right)}{\frac{1}{K_a} + \frac{2L}{D_v} + \frac{1}{K_d}}, \tag{6}$$

where the parameters A and m are constants.

Because of the solid–gas interface transfer resistance, oxygen permeation flux can be given:

In shell side:

$$J_{O_2} = K'_g\left(\frac{P'_{O_2}}{RT} - \frac{P'_{O_2 s}}{RT}\right) \tag{7}$$

In tube side:

$$J_{O_2} = K''_g\left(\frac{P''_{O_2 s}}{RT} - \frac{P''_{O_2}}{RT}\right) \tag{8}$$

where K'_g, K''_g are the oxygen transfer coefficients in the shell and tube sides, respectively.

A mass balance on oxygen gives

In tube side:

$$\frac{dP''_{O_2}}{dx} = \frac{4RTJ_{O_2}}{u_1 d_1} \tag{9}$$

In shell side:

$$\frac{dP'_{O_2}}{dx} = \frac{4RTJ_{O_2} d_2}{u_2\left(d_3^2 - d_2^2\right)}, \tag{10}$$

with the boundary conditions

$$P''_{O_2} = 0 \qquad \text{when } x = 0 \tag{11}$$

$$P'_{O_2} = 0.21 \qquad \text{when } x = 0. \tag{12}$$

Equations 6–12 were solved using the numerical method of IMSL. The parameters used for modeling the oxygen permeation are shown in Table 1. As shown, P, T are the operation condition; u_1, u_2, K', K'' are calculated from the gas flow rate and geometrical size of the tube membrane; K_a, K_d are cited from the perovskite-type $La_{0.2}Sr_{0.8}CoO_{3-\delta}$ membrane reported by Zeng and Lin (1998); and D_v, A, m are obtained from our previous study (Li et al., 1998).

The oxygen permeation flux was calculated by the following equation

$$J_{O_2} = Q_{air}\left(C''_{O_2,In} - C''_{O_2,Ou}\right), \tag{13}$$

Table 1. Parameters for Modeling the Oxygen Permeation

Parameter	Value
u_1 (cm/s)	3.70
u_2 (cm/s)	2.64
P (atm)	1
T (K)	1,123
R (atm·cm^3/mol·K)	82.06
K' (cm/s)	7.47
K'' (cm/s)	57.6
D_v (cm^2/s)	3.36×10^{-6}
K_a (cm/s)	1.38×10^{-4}
K_d (cm/s)	8.89×10^{-5}
A (mol/cm^3·atm$^{-0.02}$)	0.11
m	−0.02

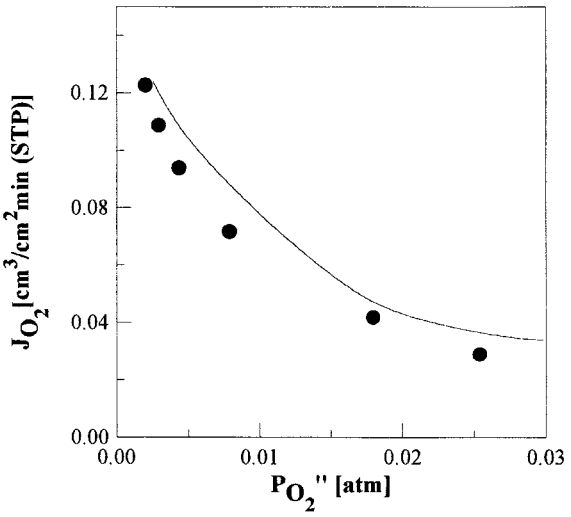

Figure 5. Pressure dependence of the oxygen flux of the tubular $La_{0.6}Sr_{0.4}Co_{0.2}Fe_{0.8}O_{3-\delta}$ membrane.
(●) experiment results; (____) modeling results.

where Q_{air} is the air flow rate, $C''_{O_2,In}$, $C''_{O_2,Ou}$ are the upstream oxygen concentration of the inlet and outlet, respectively.

Results and Discussion

Comparison of experimental and modeling results

Figure 5 shows oxygen permeation flux through the tubular $La_{0.6}Sr_{0.4}Co_{0.2}Fe_{0.8}O_{3-\delta}$ membrane at 1,123 K as a function of downstream oxygen partial pressure, P''_{O_2}. During the measurement, the oxygen partial pressure at the air sweeping side of the membrane was kept at a nearly fixed value (0.21 atm). Under these experimental conditions, the oxygen flux decreased with increasing downstream oxygen partial pressure and coincided with the results of the oxygen permeation modeling study.

Figure 6 shows oxygen permeation flux through the tubular $La_{0.6}Sr_{0.4}Co_{0.2}Fe_{0.8}O_{3-\delta}$ membrane at 1,123 K as a function of the helium flow rate. It can be seen from Figure 6 that the oxygen fluxes increase with the increase of the helium flow rate. A drastic increase in the flux was observed experimentally when the helium flow rate changes from 7.25 to 43.5 mL/min. As shown in Figure 5, when the helium flow rate changed from 7.25 to 43.5 mL/min, the oxygen partial pressure in the downstream changed from 3.6×10^{-2} to 2.9×10^{-3}. Therefore the oxygen fluxes increase drastically with the helium flow rate. For a helium flow rate varying from 43.5 to 72.5 mL/min, the oxygen partial pressure in the downstream changed from 2.9×10^{-3} to 1.5×10^{-3}, leading to a less obvious change in the oxygen permeation flux. The modeling result also proves the conclusion just mentioned.

Figure 7 shows the oxygen permeation flux through the tubular $La_{0.6}Sr_{0.4}Co_{0.2}Fe_{0.8}O_{3-\delta}$ membrane at 1,123 K as a function of air flow rate. Compared to the effects of the helium flow rate, the oxygen permeation flux remains essentially unchanged with varying air flow rate. This was because the change in the air flow rate did not cause apparent changes

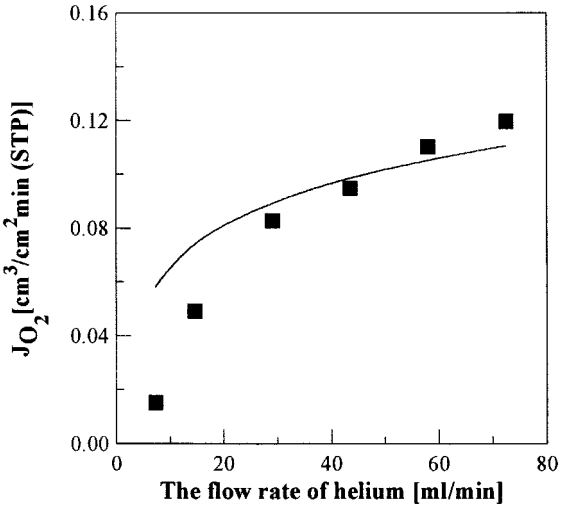

Figure 6. Helium flow-rate dependence of the oxygen flux of the tubular $La_{0.6}Sr_{0.4}Co_{0.2}Fe_{0.8}O_{3-\delta}$ membrane.

(■) experiment results; (____) modeling results.

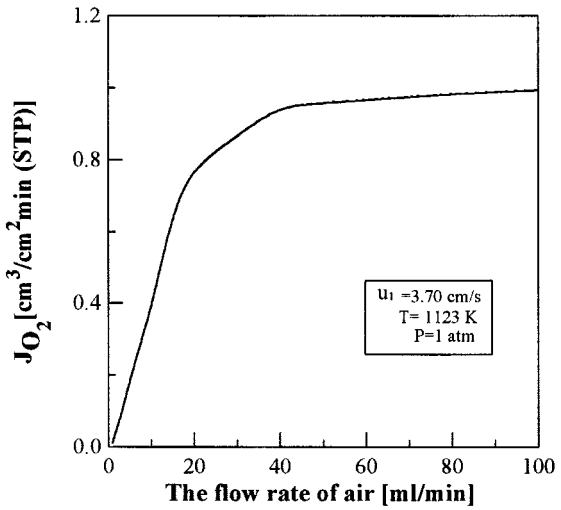

Figure 8. Modeling air flow-rate dependence of the oxygen permeability of the tubular $La_{0.6}Sr_{0.4}Co_{0.2}Fe_{0.8}O_{3-\delta}$ membrane.

in the oxygen partial pressure in the upstream. So the effect of the change of the air flow rate on the oxygen flux was negligible. It can also be seen from Figure 7 that the experimental oxygen permeation flux is lower than the results of the oxygen permeation modeling study. The cause is that the parameters of the modeling study were obtained from membranes reported in the literature (Li et al., 1998; Bouwmeester and Burggraaf, 1996; Zeng and Lin, 1998) and may be slightly discriminatory toward those of the tubular $La_{0.6}Sr_{0.4}Co_{0.2}Fe_{0.8}O_{3-\delta}$ membrane. The model results predict a decrease of the oxygen permeation flux below an air flow rate of 100 mL/min. The reason for these are discussed in the next section.

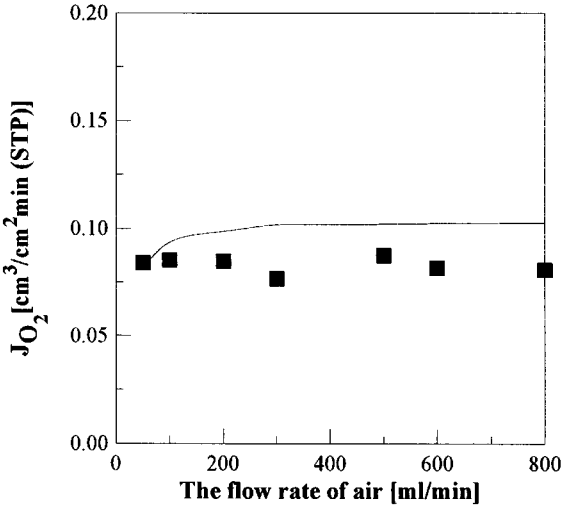

Figure 7. Air flow-rate dependence of the oxygen flux of the tubular $La_{0.6}Sr_{0.4}Co_{0.2}Fe_{0.8}O_{3-\delta}$ membrane.

(■) experiment results; (____) modeling results.

Parametric study

Figure 8 shows the modeling oxygen permeation data at 1,123 K as a function of a small air flow rate. Compared to the effects of a large air flow rate, a drastic increase in flux was predicted by a modeling study when the air flow rate changes from 1 to 40 mL/min. The results indicated that during the oxygen permeation operation, air should be supplied sufficiently.

Figure 9 shows the modeling downstream oxygen pressure data at 1,123 K as a function of the membrane length. For the membrane with oxygen vacancy concentration insensitive to oxygen partial pressure ($m = 0.02$), P''_{O_2} increases obviously with the increasing of tube length. However, for the membrane with oxygen vacancy concentration sensitive to oxygen partial pressure ($m = 0.2$), P''_{O_2} maintains a nearly

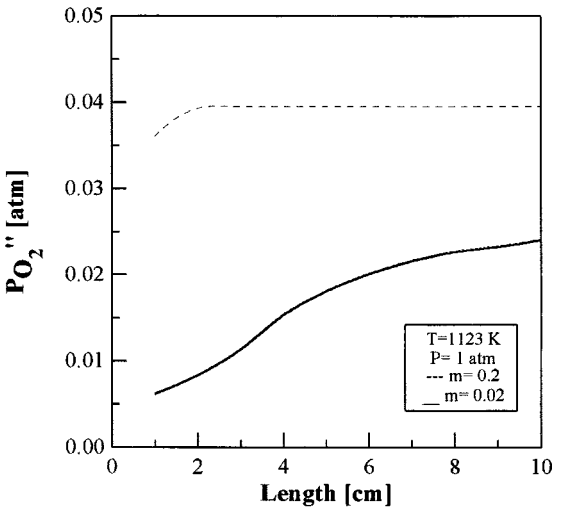

Figure 9. Influence of the tube length on the downstream oxygen partial pressure.

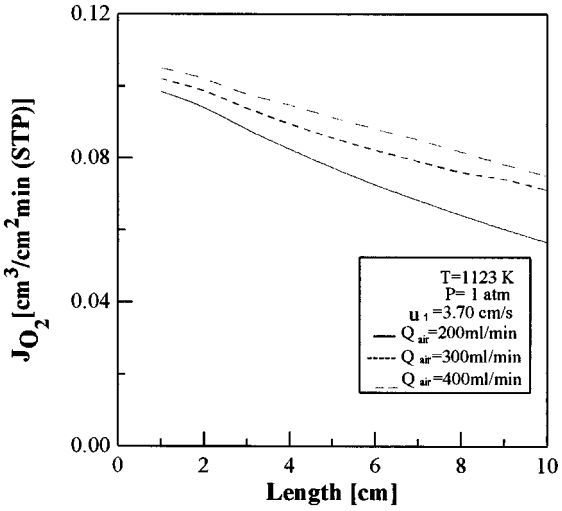

Figure 10. Influence of the tube length on the oxygen permeation flux.

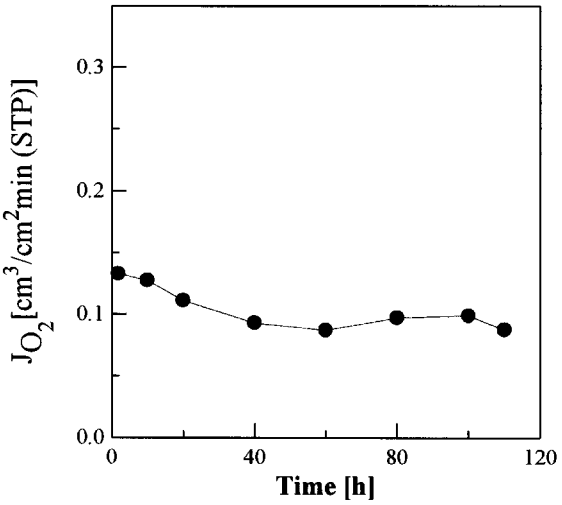

Figure 12. Oxygen flux through the tubular $La_{0.6}Sr_{0.4}Co_{0.2}Fe_{0.8}O_{3-\delta}$ membrane for long-term operation (1,123 K).

constant value along the axial length of the tubular membrane. Figure 10 shows the influence of tube length on the oxygen permeation flux ($m = 0.02$). As can be seen, for the membrane with an oxygen vacancy concentration insensitive to the oxygen partial pressure, the oxygen permeation flux decreases when the tube length increases. Increasing the air flow rate will remit the decreasing of the oxygen permeation flux.

Figure 11 shows the modeling of the oxygen permeation data of the tubular membrane at 1,123 K as a function of membrane thickness. When the membrane thickness (L) is larger than the characteristic membrane thickness (Lc), the oxygen flux varies inversely with L^n, where $n = 1$, in agreement with Wagner's theory. Lc can be obtained from Figure 11. The values are, respectively, 0.02, 0.2, and 2 mm for the membrane with an oxygen vacancy diffusivity (D_v) of 3.36×10^{-7}, 3.36×10^{-6}, 3.36×10^{-5} cm^2/s.

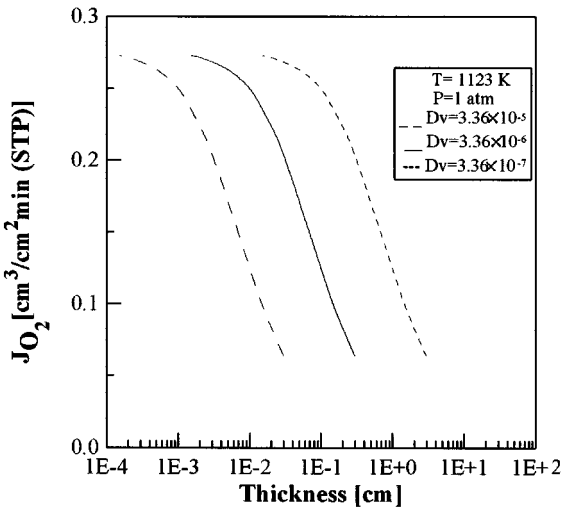

Figure 11. Influence of the membrane thickness on the oxygen permeation flux.

Membrane stability

For industrial applications, the membrane material must exhibit a long-term phase stability under the tubular membrane operating conditions. Figure 12 shows the oxygen permeating data of tubular $La_{0.6}Sr_{0.4}Co_{0.2}Fe_{0.8}O_{3-\delta}$ membrane operated for 110 h in an oxygen/nitrogen gradient at 1,123 K. The oxygen flux slightly declined after several hours of operation. Kruidhof et al. (1993) reported similar results on another perovskite-type ceramic membrane.

The elements on both the surfaces and the cross section of the membrane before and after the oxygen permeation experiment were analyzed by EDS. The results show that the composition in the cross section of the membrane after the permeation experiment is similar to that of the fresh membrane. Sulfur was found on both surfaces of the membrane after the permeation experiment. The results of XRD analysis on both the surfaces of the membrane after the oxygen permeation are shown in Figure 13. As shown, $SrSO_4$ and $CoSO_4$ are present on the membrane surface exposed to air, and $SrSO_4$ is the only sulfur-containing species on the membrane surface exposed to helium. Ten Elshof et al. (1995b) also found the presence of $SrSO_4$ on the membrane surface during oxidative coupling of methane in a mixed-conducting perovskite membrane reactor, but he did not explain the phenomenon. In this study, the origin of $SrSO_4$ and $CoSO_4$ was attributed to the interaction of a trace amount (<1000 ppm according to the purity of gas) of SO_2 in the air and the helium with the surface of the membrane.

In addition to the perovskite phase and the sulfates, the air surface of the membrane contains phases of SrO, Co_2O_3, and La_2O_3, and the helium surface contains only SrO and La_2O_3. These results show that segregation of surface elements occurred over 110 h of oxygen permeation, which is in agreement with the observation of Tsai et al. (1997) and ten Elshof et al. (1995b). Although the perovskite phase is still present on the membrane surface, the composition of the perovskite phase must be very different from the fresh membrane due to the formation of the other pure oxide phases summarized

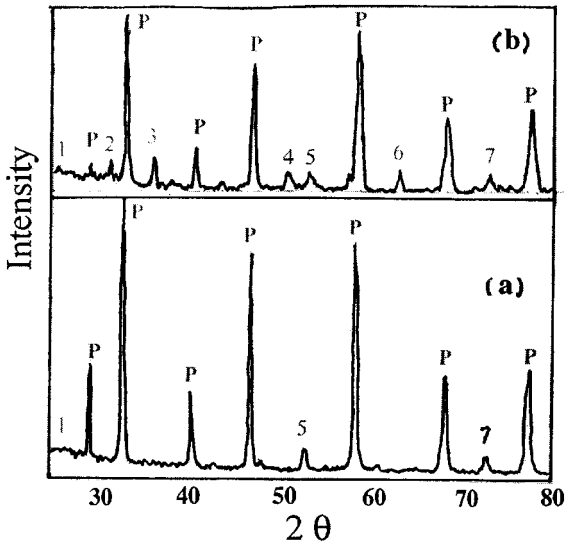

Figure 13. X-Ray diffraction patterns of tubular $La_{0.6}Sr_{0.4}Co_{0.2}Fe_{0.8}O_{3-\delta}$ membrane after 110 h oxygen permation.

Perovskite: (a) helium sweeping side surface; (b) air sweeping side surface; 1. $SrSO_4$ (002); 2. Co_2O_3 (002); 3. $SrSO_4$ (220); 4. $CoSO_4$(131); 5. SrO (220), 6. SrO (311); 7. La_2O_3 (662).

earlier.

The sulfates ($SrSO_4$ and $CoSO_4$) and the segregation products (SrO, Co_2O_3, and La_2O_3) that formed on the surfaces or in the bulk of the membrane may decrease either the rate of bulk diffusion or the surface reaction, causing a decline in the oxygen flux of $La_{0.6}Sr_{0.4}Co_{0.2}Fe_{0.8}O_{3-\delta}$ membrane. Figure 14 shows the oxygen permeation data of a tubular $La_{0.6}Sr_{0.4}Co_{0.2}Fe_{0.8}O_{3-\delta}$ membrane at 1,123 K after SO_2 in the air and helium have been removed. In comparison to the result shown in Figure 12, the oxygen permeation was stable

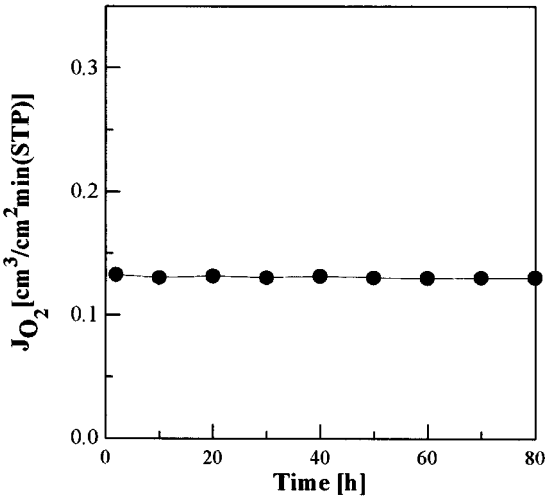

Figure 14. Oxygen permeation through the tubular $La_{0.6}Sr_{0.4}Co_{0.2}Fe_{0.8}O_{3-\delta}$ membrane for long-term operation after SO_2 in air and helium has been removed (1,123 K).

over a period of 80 h. Sulfur was not found on both surfaces of the membrane after the permeation experiment from the EDS results.

Conclusions

Tubular $La_{0.6}Sr_{0.4}Co_{0.2}Fe_{0.8}O_{3-\delta}$ perovskite-type membranes were prepared by isostatic pressing. A mathematical model was developed to simulate the performance of the tubular perovskite-type dense membranes for oxygen permeation. The experimental oxygen permeation fluxes increase with the decrease of the downstream oxygen partial pressure and the increase of the helium flow rate, which coincide with the results of the oxygen permeation modeling study.

Parametric study indicated that during the oxygen permeation, air should be supplied sufficiently. The oxygen permeation flux decreases when the tube length increases. Increasing the air flow rate will remit the decreasing of the oxygen permeation flux. The oxygen permeation flux can be increased by reducing the membrane thickness until it becomes less than a characteristic value.

The oxygen flux decreased by about 30% over 110 h of the oxygen permeation experiments. EDS and XRD analysis indicated that $SrSO_4$, $CoSO_4$, SrO, Co_2O_3, and La_2O_3 are formed on the surfaces of the tubular membranes due to interaction between trace SO_2 in the air and the helium with the surface of the membrane and segregation of surface elements. The changes on the surface chemical composition and phase structure are responsible for the decline of the oxygen permeation flux. The oxygen permeation of the tubular $La_{0.6}Sr_{0.4}Co_{0.2}Fe_{0.8}O_{3-\delta}$ membrane at 1,123 K was stable after SO_2 in air and helium was removed.

Acknowledgments

This work is supported by the National Advanced Materials Committee of China (NAMCC, No. 715-006-0120).

Literature Cited

Balachandran, U., J. T. Dusk, P. S. Maiya, B. Ma, R. L. Mieville, M. S. Kleefisch, and C. A. Udovich, "Ceramic Membrane Reactor for Converting Methane to Syngas," *Catal. Today*, **36**, 265 (1997).

Balachandran, U., J. T. Dusk, R. L. Mieville, R. B. Poeppel, M. S. Kleefisch, S. Pei, T. P. Kobylinski, C. A. Udovich, and A. C. Bose, "Dense Ceramic Membranes for Partial Oxidation of Methane to Syngas," *Appl. Catal. A: General*, **133**, 19 (1995).

Bouwmeester, H. J. M., and A. J. Burggraaf, "Dense Ceramic Membranes for Oxygen Separation," *Fundamentals of Inorganic Membrane Science and Technology*, A. J. Burggraaf and L. Cot, eds., Elsevier, Amsterdam, p. 435 (1996).

Bouwmeester, H. J. M., and A. J. Burggraaf, "Dense Ceramic Membranes for Oxygen Separation," *CRC Handbook of Solid State Electrochemistry*, Chap. 14, H. J. M. Bouwmeester, ed., Elsevier, Amsterdam (1997).

Chen, C. H., H. J. M. Bouwmeester, R. H. E. van Doorn, H. Kruidhof, and A. J. Burggraaf, "Oxygen Permeation of $La_{0.3}Sr_{0.7}CoO_{3-\delta}$," *Solid State Ionics*, **98**, 7 (1997).

Gur, T. M., A. Belzner, and R. A. Huggins, "A New Class of Oxygen Selective Chemically Driven Nonporous Ceramic Membrane: Part I. A Site Doped Perovskites," *J. Memb. Sci.*, **75**, 151 (1992).

Hsieh, H. P., *Inorganic Membrane for Separation and Reaction*, Elsevier, Amsterdam (1996).

Itoh, N., T. Kato, K. Uchida, and K. Haraya, "Preparation of Pore-Free Disk of $La_{1-x}Sr_xCoO_3$ Mixed Conductor and Its Oxygen Permeability," *J. Memb. Sci.*, **92**, 239 (1994).

Kawada, T., T. Horita, N. Sakai, Y. Yokokawa, and M. Dokiya, "Experimental Determination of Oxygen Permeation Flux through Bulk and Grain Boundary of $La_{0.7}Ca_{0.3}CrO_3$," *Solid State Ionics*, **79**, 201 (1995).

Kharton, V. V., E. N. Naumovich, and A. V. Nikolaev, "Materials of High-Temperature Electrochemical Oxygen Membranes," *J. Memb. Sci*., **111**, 149 (1996).

Kruidhof, H., H. J. M. Bouwmeester, R. H. E. v. Doom, and A. J. Burggraaf, "Influence of Order-Disorder Transitions on Oxygen Permeability Through Selected Nonstoichiometric Perovskite-Type Oxides," *Solid State Ionics*, **63–65**, 816 (1993).

Lee, T. H., Y. L. Yang, A. J. Jacobsen, B. Abeles, and M. Zhou, "Oxygen Permeation in Dense $SrCo_{0.8}Fe_{0.2}O_{3-d}$ Membranes: Surface Exchange Kinetics Versus Bulk Diffusion," *Solid State Ionics*, **100**, 77 (1997).

Li, S., W. Jin, P. Huang, N. Xu, J. Shi, and Y. S. Lin, "Tubular Lanthanum Cobaltite Perovskite Type Membrane for Oxygen Permeation," *J. Memb. Sci*. (1998).

Li, S., W. Jin, P. Huang, N. Xu, J. Shi, M. Z.-C. Hu, E. A. Payzant, and Y. H. Ma, "Perovskite-Related ZrO_2-Doped $SrCo_{0.4}Fe_{0.6}O_{3-\delta}$ Membrane for Oxygen Permeation," *AIChE J.*, **45**, 276 (1999a).

Li, S., W. Jin, P. Huang, N. Xu, J. Shi, Y. S. Lin, M. Z.-C. Hu, and E. A. Payzant, "Comparison of Oxygen Permeability and Stability of Perovskite $La_{0.2}A_{0.8}Co_{0.2}Fe_{0.8}O_{3-\delta}$ (A = Sr, Ba, Ca) Membranes," *Ind. Eng. Chem. Res*., **38**, 2963 (1999b).

Lin, Y. S., and Y. Zeng, "Catalytic Properties of Oxygen Semipermeable Perovskite Type Ceramic Membrane Materials for Oxidative Coupling of Methane," *J. Catal*., **164**, 220 (1996).

Lin, Y. S., W. Wang, and J. Han, "Oxygen Permeation Through Thin Mixed-Conducting Solid Oxide Membrane," *AIChE J.*, **40**, 786 (1994).

Mizusaki, J., Y. Mima, S. Yamauchi, K. Fukei, and H. Tagawa, "Nonstoichiometry of the Perovskite-Type Oxides $La_{1-x}Sr_xCoO_{3-\delta}$," *J. Solid State Chem*., **80**, 102 (1989).

Qiu, L., T. H. Lee, L.-M. Liu, Y. L. Yang, and A. J. Jacobson, "Oxygen Permeation Studies of $SrCo_{0.8}Fe_{0.2}O_{3-\delta}$," *Solid State Ionics*, **76**, 321 (1995).

Stevenson, J. W., T. R. Armstrong, R. D. Carmeim, L. R. Pederson, and W. J. Weber, "Electrochemical Properties of Mixed Conducting Perovskites $La_{1-x}M_xCo_{1-y}Fe_yO_{3-\delta}$ (M = Sr, Ba, Ca)," *J. Electrochem. Soc*., **143**, 2722 (1996).

ten Elshof, J. E., B. A. Van Hassel, and H. J. M. Bouwmeester, "Activation of Methane Using Solid Oxide Membrane," *Catal. Today*, **25**, 397 (1995a).

ten Elshof, J. E., H. J. M. Bouwmeester, and H. Verweij, "Oxidative Coupling of Methane in a Mixed-Conducting Perovskite Membrane Reactor," *Appl. Catal. A: General*, **130**, 195 (1995b).

ten Elshof, J. E., H. J. M. Bouwmeester, and H. Verweij, "Oxygen Transport Through $La_{1-x}Sr_xFeO_{3-\delta}$ Membranes. I. Permeation in Air/He Gradients," *Solid State Ionics*, **81**, 97 (1995c).

Teraoka, Y., H. M. Zhang, S. Furukawa, and N. Yamazoe, "Oxygen Permeation through Perovskite-Type Oxides," *Chem. Lett*., 1743 (1985).

Tsai, C.-Y., A. G. Dixon, W. R. Moser, and Y. H. Ma, "Dense Perovskite Membrane Reactors for the Partial Oxidation of Methane to Syngas," *AIChE J.*, **43**, 2741 (1997).

van Hassel, B. A., J. E. ten Elshof, and H. J. M. Bouwmeester, "Oxygen Permeation Flux Through $La_{1-y}Sr_yFeO_{3-\delta}$ Limited by Carbon Monoxide Oxidation Rate," *Appl. Catal. A: General*, **119**, 279 (1994).

van Hassel, B. A., T. Kawada, N. Sakai, H. Yokohana, and M. Dokiya, "Oxygen Permeation Modeling of $La_{1-y}Ca_yCrO_{3-\delta}$," *Solid State Ionics*, **61**, 41 (1993a).

van Hassel, B. A., T. Kawada, N. Sakai, H. Yokohana, and H. J. M. Bouwmeester, "Oxygen Permeation Modeling of Perovskites," *Solid State Ionics*, **66**, 295 (1993b).

Xu, S. J., and W. J. Thomson, "Stability of $La_{0.6}Sr_{0.4}Co_{0.2}Fe_{0.8}O_{3-\delta}$ Perovskite Membrane in Reducing and Nonreducing Environments," *Ind. Eng. Chem. Res*., **37**, 1290 (1998).

Zeng, Y., Y. S. Lin, and S. L. Swartz, "Perovskite Type Ceramic Membranes: Synthesis, Oxygen Permeation and Membrane Reactor Performance for Oxidative Coupling of Methane," *J. Memb. Sci*., **150**, 687 (1998).

Zeng, Y., and Y. S. Lin, "A Transient TGA Study on Oxygen Permeation Properties of Perovskite Type Ceramic Membrane," *Solid State Ionics*, **110**, 209 (1998).

Manuscript received Feb. 22, 1999, and revision received July 8, 1999.